Synthesis of (η^3-Allyl)bromodicarbonylbis(pyrazole)molybdenum(II) and Reactivity towards [Au(acac)PPh_3]: Structure and Dynamic Behavior of the Monometallic Pyrazole and Heterometallic Pyrazolate Complexes

Paloma Paredes,[a] Daniel Miguel,[a] and Fernando Villafañe*[a]

Keywords: Molybdenum / Gold / Heterometallic complexes / N ligands / Fluxionality

The reactions of [Mo(η^3-allyl)Br$(CO)_2(NCMe)_2$] and two equivalents of Hpz (pyrazole) or Hdmpz (3,5-dimethylpyrazole) lead to [Mo(η^3-allyl)Br$(CO)_2(Hpz)_2$] or [Mo(η^3-allyl)Br$(CO)_2(Hdmpz)_2$]. The Hpz and Hdmpz ligands are coordinated *cis* and *trans* with respect to the allyl group in the solid state, whereas in their solutions a slow trigonal twist process is detected. These complexes react with Tl(acac) giving [Mo(acac)(η^3-allyl)$(CO)_2$(Hpz)] and [Mo(acac)(η^3-allyl)$(CO)_2$(Hdmpz)], which also undergo a slow trigonal twist process in solution. The latter complex may also be obtained by the reaction of equimolar amounts of [Mo(η^3-allyl)Br$(CO)_2(Hdmpz)_2$] and [Au(acac)PPh_3], giving [Au$BrPPh_3$] as a by product. The reaction of these molybdenum acac complexes with [Au(acac)PPh_3] give rise to the heterobimetallic bridging pyrazolate complexes [Mo(acac)(η^3-allyl)$(CO)_2$(μ-pz)AuPPh_3] and [Mo(acac)(η^3-allyl)$(CO)_2$(μ-dmpz)AuPPh_3]. The solid state structure of the latter, which is also obtained from [Mo(η^3-allyl)Br$(CO)_2(Hdmpz)_2$] and two equivalents of [Au(acac)PPh_3], with [Au$BrPPh_3$] as a by product, reveals the coordination of the bridging dimethylpyrazolate ligand *trans* to the allyl group. Two different dynamic processes which are slowed down at low temperatures are detected in solution for each heterobimetallic complex: trigonal twist for the pyrazolate bridging complex, and hindered rotation of the Mo–N bond for the more hindered dimethylpyrazolate complex.

Introduction

Pyrazolate ligands are commonly used as bridging ligands since they allow for the study of the bimetallic moiety, holding both metals in close proximity but at the same time being flexible enough to adopt different geometries with a wide variety of metals.[1] The interest of these studies embraces different fields, such as the physical properties and the biological activity of new complexes, or their unusual chemical behavior and catalytic activity.[2]

The bridging pyrazolate heterobimetallic complexes are of special interest, and may be obtained by deprotonation of a terminal pyrazole complex when a second metallic substrate is present. This strategy allows the systematic synthesis of heterobimetallic systems, as has been successively used by different groups, mainly with middle and late transition elements.[3] Herein we report on the synthesis of molybdenum(II) complexes containing two terminal pyrazoles coordinated in a *cis* manner. We also present the first results of the use of these compounds as precursors for heterobimetallic systems: deprotonation of the pyrazole ligands, and further coordination to a late transition metal would lead to the synthesis of early-late bimetallic complexes. These are particularly interesting in the field of heterobimetallic systems, as the clear differences between both metals enhance the synergism responsible for their improved activity.[4]

Results and Discussion

Synthesis and Characterization of [MoBr(η^3-allyl)$(CO)_2(Hpz)_2$] and [MoBr(η^3-allyl)$(CO)_2(Hdmpz)_2$]

The reactions of [MoBr(η^3-allyl)$(CO)_2(NCMe)_2$] with a two-fold excess of pyrazole (Hpz) or dimethylpyrazole (Hdmpz) in dichloromethane are instantaneous at room temperature affording [MoBr(η^3-allyl)$(CO)_2(Hpz)_2$] (**1a**) and [MoBr(η^3-allyl)$(CO)_2(Hdmpz)_2$] (**1b**), respectively, isolated as yellow crystalline solids.

There are two possible geometries for these complexes, as depicted in Figure 1. They are pseudo-octahedral if the η^3-allyl ligand is considered as occupying one coordination po-

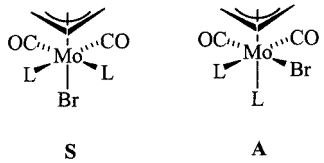

Figure 1. Two possible structures for complexes [MoBr(η^3-allyl)$(CO)_2L_2$]

[a] Departamento de Química Inorgánica, Facultad de Ciencias, Universidad de Valladolid, 47005 Valladolid, Spain

sition, having its terminal atoms oriented over the carbonyl groups, as has been demonstrated to be the most energetically favorable arrangement.[5] The two possible geometries are: **S** or symmetric, where the pyrazoles are coordinated in the *equatorial* positions, *trans* to the carbonyls; and **A** or asymmetric, where one of the pyrazoles is coordinated *trans* to the allyl group, in the *axial* position (Figure 1).

The NMR spectra provide very useful information for identifying the geometry of the complex, since both pyrazoles and both methylenes of the allyl group are equivalent in the symmetric isomer **S**, but inequivalent in the asymmetric isomer **A**. The latter is the only isomer detected in the ^1H and $^{13}C\{^1H\}$ NMR spectra of **1a** and **1b** at room temperature. However, some of the signals in the ^1H NMR spectra are broad, which might be a consequence of a slow exchange process before the coalescence.

These complexes $[MoX(\eta^3\text{-allyl})(CO)_2L_2]$ (X = halide or pseudo halide, L_2 = two monodentate ligands or a bidentate ligand) usually display a nondissociative trigonal twist process in which there is an intramolecular rotation of the XL_2 triangular face,[6] which would lead to the equilibrium depicted in Scheme 1. The isomers involved in this equilibrium are the symmetric **S** and both enantiomers of the asymmetric **A**. Therefore, if this exchange process is fast enough, a symmetric average spectrum should be observed.

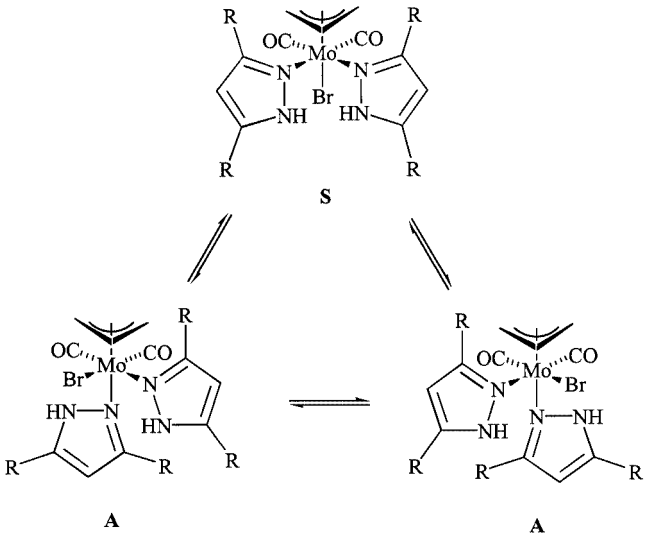

Scheme 1. Trigonal twist process observed for **1a** (R = H) and **1b** (R = CH_3)

Other dynamic processes in solution have been detected for these types of complexes, such as the $\eta^3-\eta^1-\eta^3$ rearrangement of the allyl,[7] or the recently described "pivoted double switch" process, where the *axial* ligand remains in the same position, while the bromo and the other ligand *trans* to the carbonyls switch between both *equatorial* positions.[8] The $\eta^3-\eta^1-\eta^3$ rearrangement of the allyl would render the H^{anti} and H^{syn} equivalent, giving an A_4X pattern for the allyl group in the ^1H NMR spectra. On the other hand, the "pivoted double switch" mechanism would never render both pyrazole ligands equivalent, since the pyrazole in the *axial* position would not exchange with the other pyrazole.

A variable temperature ^1H NMR spectroscopic study was carried out in order to understand the exact nature of the process in solution that leads to the broadening of the signals observed in the ^1H NMR spectra at room temperature for **1a** and **1b**.

The ^1H NMR spectrum of **1a** at 333 K shows signals due to a symmetric dynamic situation where both pyrazoles are equivalent, thus confirming the trigonal twist exchange process which is very slow at room temperature. On the other hand, a symmetric situation appears when the ^1H NMR spectrum of **1b** is recorded at 353 K in C_6D_6, as some of the signals of the different Hdmpz groups coincide, as well as those of different halves of the allyl group (see Exp. Sect.). Hence, the same trigonal twist exchange process is proposed for **1b**, but is slower than that of **1a**. This is in accordance with the higher steric requirements of Hdmpz compared with Hpz.

The allyl protons H^{anti} and H^{syn} always remain inequivalent, and the pyrazole ligands are equivalent when the processes are fast, which leads to both the $\eta^3-\eta^1-\eta^3$ rearrangement of the allyl and the "pivoted double switch" process being discarded.

Only the asymmetric isomer is detected in the ^1H NMR spectra of both complexes at low temperatures, indicating that the equilibrium occurs between the two asymmetric enantiomers **A** depicted in Scheme 1. The symmetric isomers **S** are not observed for any of the two complexes, which suggests that they are energetically very unfavorable.

The ^1H NMR spectra recorded at low temperatures display sharp signals. The H^4 signals in **1a** are pseudo quadruplets, due to coupling with the rest of pyrazolic protons including the pyrrolic proton, as was confirmed from selective homodecoupling experiments. Therefore, the broadness observed at room temperature might then also be due to a rapid prototropic exchange involving the pyrrolic proton, which is common in pyrazole complexes.[9] The homodecoupling experiments carried out on **1a** at low temperature allowed us to unequivocally assign the signals of the pyrazolic hydrogens. However, this assignment cannot be extended to the rest of the complexes described here, since the chemical shifts of the hydrogens or methyl groups in positions 3 and 5 seem to be affected by different factors, which are difficult to evaluate: whether the hydrogen (or methyl) group at position 3 resonates at a higher field than at position 5 or vice versa may vary in the same family of complexes,[3g] or even depend on the solvent used.[10] Therefore, the assignment proposed for the rest of the complexes in the Experim. Section may be considered as tentative.

The IR spectra of both complexes show two bands in the C−O stretching region in solution, although more bands are detected in the solid state. This is a common feature in carbonyl complexes and is attributed to the lower symmetry of the molecule in the crystal compared to the isolated molecule in solution. The C−O frequencies are slightly higher for **1a** than for **1b** when the IR is recorded in solution. This is to be expected considering that Hdmpz is a better donor

than Hpz, and is also observed for the rest of the complexes described in this work. However, the C−O frequencies of **1a** in the solid state are appreciably lower than those of **1b** (see Exp. Sect.). This has no immediate explanation, as the rest of the analytical and spectroscopic data are in accordance with the proposed geometries. Thus, we decided to carry out an X-ray study of both complexes in order to also obtain crystallographic data, and thus to determine whether this could shed some light on these anomalous frequencies.

The structures are shown in Figure 2 and relevant distances and angles are collected in Table 1. As indicated above, the molybdenum atoms are pseudo-octahedrally coordinated, assuming that the allyl groups occupy one site. The two carbonyls and the allyl group show the expected orientation, already described.[5,11] As evidenced by Table 1, the distances and angles are very similar in both complexes, and similar to those found in the previously reported structure of a bromodicarbonylmolybdenum(II) complex with pyrazole and phenylallyl.[12] It should be noted that one of the pyrazole ligands is coordinated *trans* to the allyl group in all three structures (asymmetric isomer **A** in Scheme 1), opposite to what is usually found in complexes of the type [MoX(η^3-allyl)$(CO)_2L_2$] (X = halide or pseudo halide, L_2 = nitrogen donor ligand), where the nitrogen donor ligands are always *trans* to the carbonyl groups (**S** isomer).[11]

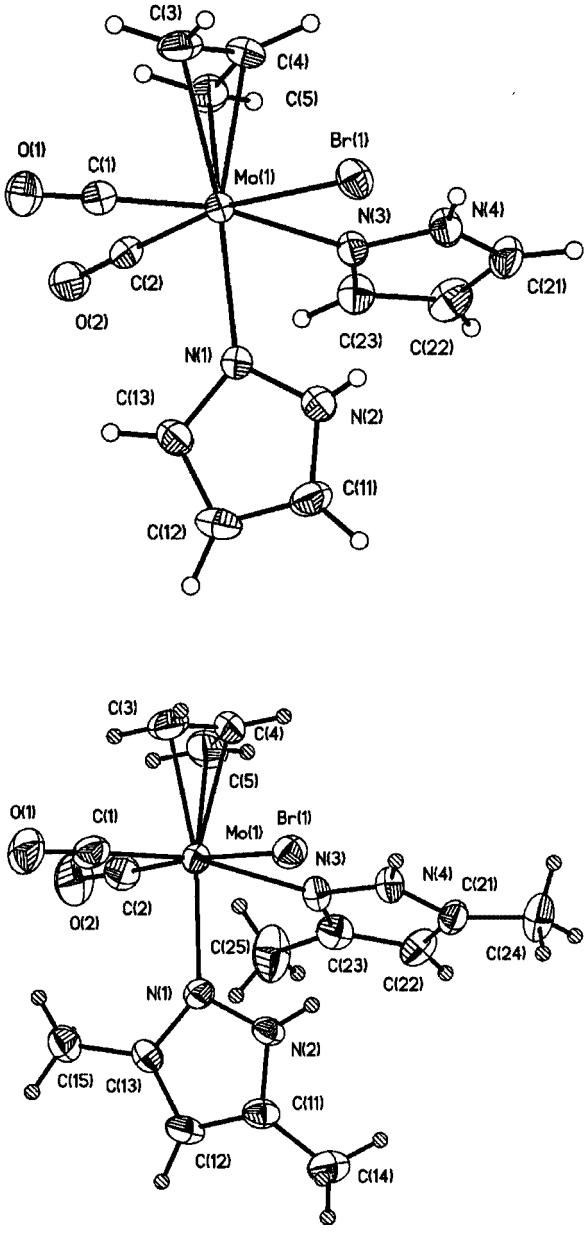

Figure 2. Perspective views of [Mo(η^3-allyl)$Br(CO)_2(Hpz)_2$], **1a** (above), and [Mo(η^3-allyl)$Br(CO)_2(Hdmpz)_2$], **1b** (below), showing the atom numbering

Table 1. Selected distances [Å] and angles [deg.] for [Mo(η^3-allyl)-$Br(CO)_2(Hpz)_2$] (**1a**) and [Mo(η^3-allyl)$Br(CO)_2(Hdmpz)_2$] (**1b**)

	1a	**1b**
Mo(1)−C(2)	1.940(3)	1.932(5)
Mo(1)−C(1)	1.957(3)	1.948(5)
Mo(1)−C(4)	2.215(3)	2.206(4)
Mo(1)−N(1)	2.222(2)	2.241(3)
Mo(1)−N(3)	2.268(2)	2.304(3)
Mo(1)−C(3)	2.325(3)	2.345(4)
Mo(1)−C(5)	2.338(3)	2.346(4)
Mo(1)−Br(1)	2.738(1)	2.771(1)
C(1)−O(1)	1.151(4)	1.160(4)
C(2)−O(2)	1.132(3)	1.160(5)
C(3)−C(4)	1.397(4)	1.396(6)
C(4)−C(5)	1.400(4)	1.381(6)
C(2)−Mo(1)−C(1)	80.06(12)	79.89(17)
C(2)−Mo(1)−N(1)	87.53(10)	91.27(15)
C(1)−Mo(1)−N(1)	90.33(10)	89.29(15)
C(2)−Mo(1)−N(3)	94.49(10)	99.27(14)
C(1)−Mo(1)−N(3)	169.26(10)	168.20(15)
N(1)−Mo(1)−N(3)	80.13(8)	78.95(11)
C(2)−Mo(1)−C(3)	107.15(13)	103.59(17)
C(1)−Mo(1)−C(3)	67.87(12)	68.76(19)
N(1)−Mo(1)−C(3)	150.34(10)	150.34(16)
N(3)−Mo(1)−C(3)	122.79(10)	122.54(16)
C(2)−Mo(1)−Br(1)	169.63(8)	172.85(12)
C(1)−Mo(1)−Br(1)	100.16(9)	95.11(12)
N(1)−Mo(1)−Br(1)	82.10(6)	83.52(8)
N(3)−Mo(1)−Br(1)	83.53(6)	84.58(8)

The Mo−C and C−O distances in the structures of **1a** and **1b** follow the expected sequence: those *trans* to the bromo ligand [C(1)−O(1)] are similar in both structures, whereas those *trans* to the pyrazoles are slightly different: C(2)−O(2) distance in **1a** is 1.132(3) Å vs. 1.160(5) Å in **1b**. This indicates that the C−O bond is stronger in **1a**, inferring that Hdmpz is a better donor than Hpz, as predicted. However, this result is difficult to rationalize with the frequencies observed from the solid-state IR spectra, which point to the opposite, since they are lower for **1a**. This feature might be explained considering lattice effects, since different space groups are detected for each molecular packing, and this should affect the C−O frequencies. This frequency anomaly might also be explained considering the short intermolecular distances where the oxygen atoms of the carbonyl groups are involved, as is discussed below.

The pyrrolic hydrogens in the structures of these two complexes are involved both in both intramolecular and in-

termolecular hydrogen bonds. The intramolecular hydrogen bonds affect the bromine atoms: 2.51 and 2.62 Å are found in **1a**, and 2.51 and 2.74 Å in **1b**, for Br(1)···H(4) and Br(1)···H(2), respectively. These distances are typical of weak hydrogen bonds,[13] and are always shorter those between the bromine atom and the pyrrolic hydrogen in the *equatorial* position. Similar hydrogen bond lengths have been found for other bromo complexes containing pyrazoles.[14]

The intermolecular hydrogen bonds involving the pyrrolic atoms clearly differ in both complexes: in **1a**, the acceptor atoms are the oxygens of the carbonyls giving distances expected for weak hydrogen bonds [H(2)···O(1) 2.75 Å, H(4)···O(2) 2.39 Å],[13] whereas no intermolecular interaction is observed for the pyrrolic hydrogens of **1b**. As indicated above, either the lattice effects or this feature (or both) might be responsible for the observed decrease in the C−O stretching frequencies in the solid IR for **1a**, since this interaction is only detected in this complex.

Acac Complexes

Once the two precursors needed to obtain heterobimetallic complexes had been synthesized, we decided to explore their reactivity towards different bases in order to deprotonate the pyrazoles and then react this pyrazolate complex with a second metal fragment. However, the treatment of either **1a** or **1b** with K_2CO_3, NEt_3, NaH, or KOH gave unchanged starting material or mixtures of unidentifiable products after forcing the conditions. This can be easily be explained in terms of the fact that these bases may act as nucleophiles, and the attack of nucleophiles on coordinated η^3-allyl groups is well-known. For [MoX(η^3-allyl)$(CO)_2L_2$] complexes, these reactions do not always afford the expected olefin,[15] but may lead to the substitution of the coordinated halogen by the nucleophile,[16] or even to decomposition.[17]

An alternative way of obtaining heterobimetallic complexes was the use of a base already coordinated to the metal fragment that was to be introduced. This fragment could immediately trap the pyrazolate formed by coordination to the second metal fragment. Thus, [Au(acac)PPh_3] was used, since the acetylacetonate could act as a base. Other acac complexes have previously been used for this purpose.[3a−3c]

The reaction of **1b** with a two-fold excess of [Au(acac)PPh_3] occurs at room temperature for 1 h in THF, and allows for the isolation of [Mo(acac)(η^3-allyl)$(CO)_2$(μ-dmpz)$AuPPh_3$] (**3b**) after separating [$AuBrPPh_3$] as a white solid by crystallization [Equation (1)]:

[MoBr(η^3-allyl)$(CO)_2$(Hdmpz)$_2$] (**1b**) + 2 [Au(acac)PPh_3] → [Mo(acac)(η^3-allyl)$(CO)_2$(μ-dmpz)$AuPPh_3$] (**3b**) + [$AuBrPPh_3$] + Hdmpz + Hacac (1)

As inferred from Equation (1), one equivalent of acac acts as a ligand, substituting one dimethylpyrazole and the bromo ligands, whereas the second acts as a base, removing the pyrrolic hydrogen and coordinating the pyrazolate ligand to the liberated "$AuPPh_3$" fragment. This sequence should coincide with the path followed by the reaction, since the products detected when the reaction was repeated using equimolar amounts of the reactants were [Mo(acac)(η^3-allyl)$(CO)_2$(Hdmpz)] (**2b**) and [$AuBrPPh_3$] [Equation (2)].

[MoBr(η^3-allyl)$(CO)_2$(Hdmpz)$_2$] (**1b**) + [Au(acac)PPh_3] → [Mo(acac)(η^3-allyl)$(CO)_2$(Hdmpz)] (**2b**) + [$AuBrPPh_3$] + Hdmpz (2)

This result led us to propose a more logical synthetic path in order to obtain these two new complexes: (a) the substitution of the bromo and pyrazole ligands by acetylacetonate was carried out with Tl(acac) instead of [Au(acac)PPh_3], and (b) this gold complex was used for the deprotonation of the remaining pyrazole and formation of the heterobimetallic complexes.

The reaction of Tl(acac) with equimolar amounts of **1a** or **1b** in dichloromethane at room temperature yielded, after separating TlBr as a precipitate, [Mo(acac)(η^3-allyl)$(CO)_2$(Hpz)] (**2a**) or [Mo(acac)(η^3-allyl)$(CO)_2$(Hdmpz)] (**2b**). The second equivalent of Hpz or Hdmpz liberated in the reaction remained in the mother liquor.

The allyl and acac signals in the ^{1}H NMR spectra of **2a** and **2b** at room temperature are indicative of a symmetric situation with respect to the plane that bisects the allyl and contains the metal atom. However some signals are broad, as occurred for complexes **1**, what is indicative of a dynamic process in solution. The ^{1}H NMR spectra at lower temperatures show signals of two isomers: one symmetric and one asymmetric, the ratio of the latter increasing as the temperature decreases. This is again in accordance with a trigonal twist process between the possible stereoisomers shown in Scheme 2. Contrarily to complexes **1**, the symmetric isomers **S** are detected in the solutions of complexes **2** (their ratio being higher as the temperature rises) which is indicative of their higher stability in this case.[18] The signals for both isomers are clearly differentiated in the $^{13}C\{^1H\}$ NMR spectra at 233 K of **2a** and **2b**.

The IR spectra of complexes **2a** and **2b** show two absorptions in the C−O stretching region, those of **2a** being slightly higher, as should be expected given the lower neat donor character of Hpz compared with Hdmpz. Another interesting feature is the N−H stretching bands, which show an important decrease for **2a**: 3159 cm^{-1}, vs. ca. 3300 cm^{-1} for **1a** and **1b**, or 3396 cm^{-1} for **2b**. In addition to this low frequency, the N−H stretching absorption observed for **2a** is very broad, which suggests that this hydrogen bond is stronger than those in complexes **1** and **2a**, which show sharp absorptions. These two factors point to a moderate hydrogen bond in **2a**, whereas those detected in the other complexes herein may be considered to be weak, as indicated above.[12,19]

Once acac has been incorporated to the molecules, they may be deprotonated to obtain the pyrazolate bridging het-

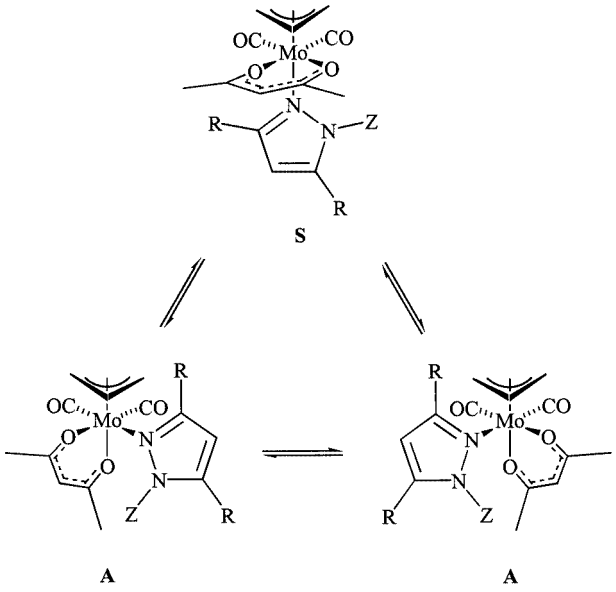

Scheme 2. Trigonal twist process observed for **2a** (R = H, Z = H), **2b** (R = CH_3, Z = H), and **3a** (R = H, Z = $AuPPh_3$).

erobimetallic complexes. The reactions of **2a** or **2b** with the equimolar amounts of [Au(acac)PPh_3] occur in 5 minutes at room temperature and in THF as the solvent, to give [Mo(acac)(η^3-allyl)$(CO)_2$(μ-pz)$AuPPh_3$] (**3a**) and [Mo(acac)(η^3-allyl)$(CO)_2$(μ-dmpz)$AuPPh_3$] (**3b**) as orange crystalline solids.

The IR spectra of **3a** and **3b** show two C−O absorptions, their frequencies being once again slightly higher for the Hpz complex, and no N−H bands are detected. Their ^{1}H NMR spectra at room temperature show allyl and acac signals indicative of a symmetric situation respect to the plane which bisects the allyl and contains the metal atom. The $^{31}P\{^1H\}$ NMR spectra show only one singlet at room temperature, whereas no $^{13}C\{^1H\}$ NMR spectra could be recorded due to the low solubility of the complexes. In this case, **3a** and **3b** showed different behavior when the variable temperature NMR spectroscopic study was carried out.

The behavior of **3a** at lower temperatures is similar to that described above for **2a**, since two isomers are detected, symmetric and asymmetric, although this time the ratio of the latter increases as the temperature decreases. This is observed both in the ^{1}H and $^{31}P\{^1H\}$ NMR spectra at low temperatures, and supports again a trigonal twist process between isomer **S** and the two enantiomers of isomer **A**, as shown in Scheme 2.

On the other hand, the $^{31}P\{^1H\}$ NMR spectra of **3b** at 213 K displays six singlets, one of them clearly more intense than the others. The ^{1}H NMR spectra at low temperature also show a major isomer with inequivalent halves for the acac and allyl ligands, and a mixture of minor isomers, although not all their signals could be completely interpreted due to their low ratio.

An X-ray diffractometric study was carried out in order to identify which isomer crystallizes. The result of this determination is shown in Figure 3, whereas Table 2 contains the more relevant distances and angles. The usual pseudo-octahedral geometry of (η^3-allyl)molybdenum complexes is found, with the open face of the allyl moiety oriented over the carbonyls. The acac ligands occupy the *equatorial* positions, whereas the *axial* position is occupied by the dimethylpyrazolate, which bridges the molybdenum and the gold atoms. The plane defined by the bridging pyrazole and the gold atom lies nearly perpendicular [91.4(1)°] to the plane defined by Mo, N(2), and the central atoms of the allyl and acac ligands [C(9) and C(5), respectively], which bisects the molybdenum complex.

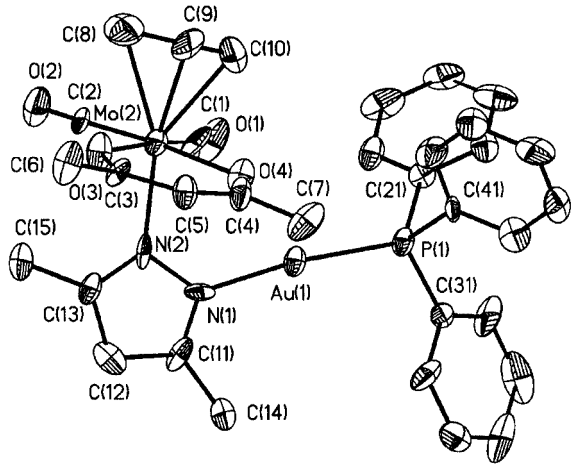

Figure 3. Perspective view of [Mo(acac)(η^3-allyl)$(CO)_2$(μ-dmpz)$AuPPh_3$] (**3b**) showing the atom numbering (the hydrogen atoms have been omitted for clarity)

The distances and angles of the "Mo(acac)(η^3-allyl)$(CO)_2$" moiety are very similar to those found in the structure of the complex [Mo(acac)(η^3-allyl)$(CO)_2$(py)],[20] where the acac also occupies the *equatorial* positions. The Au−N and Au−P distances [1.976(18) and 2.20(5) Å] are in the lower range of those previously reported for phosphanepyrazolylgold complexes [2.06(2) and 2.231(5)−2.334(5) Å, respectively].[21] The P−Au−N angle [171.9(6)°] is also in the lower limit with respect to those previously described [174.3(4)−178.0(5)°].[21]

Once the isomer in the solid state had been identified, the next step was to assign its signals in the NMR spectra. Therefore, the crystals were mixed with frozen $CDCl_3$ at 195 K, and the NMR spectra were recorded immediately after the solvent melted at 213 K. The ^{1}H and $^{31}P\{^1H\}$ NMR spectra show signals that correspond to the above mentioned major isomer. Small signals due to the minor isomers appear and increase as the solution is maintained at low temperature, until finally the same spectra as that described above, obtained when the solution was prepared at room temperature, is observed.

Hence, the isomer detected in the solid state is that labeled **S** in Scheme 2, but the $AuPPh_3$ moiety makes the plane bisecting the acac and the allyl ligands no longer a symmetry plane. This explains why its ^{1}H NMR spectrum shows inequivalent halves for the acac and allyl ligands, and suggests that the rotation of the Mo−N bond has been

Table 2. Selected distances [Å] and angles [deg.] for [Mo(acac)(η^3-allyl)$(CO)_2$(μ-dmpz)$AuPPh_3$] (**3b**)

Mo(2)−C(2)	1.89(2)
Mo(2)−C(1)	1.97(2)
Mo(2)−C(9)	2.10(3)
Mo(2)−N(2)	2.13(2)
Mo(2)−O(3)	2.148(14)
Mo(2)−O(4)	2.158(14)
Mo(2)−C(10)	2.32(2)
Mo(2)−C(8)	2.34(2)
Au(1)−N(1)	1.976(18)
Au(1)−P(1)	2.209(5)
C(1)−O(1)	1.14(2)
C(2)−O(2)	1.18(2)
O(3)−C(3)	1.22(2)
O(4)−C(4)	1.22(3)
C(8)−C(9)	1.31(3)
C(9)−C(10)	1.24(3)
C(2)−Mo(2)−C(1)	77.7(8)
C(2)−Mo(2)−C(9)	101.3(10)
C(1)−Mo(2)−C(9)	98.2(12)
C(2)−Mo(2)−N(2)	95.0(8)
C(1)−Mo(2)−N(2)	87.9(8)
C(9)−Mo(2)−N(2)	163.5(9)
C(2)−Mo(2)−O(3)	96.1(7)
C(1)−Mo(2)−O(3)	171.3(8)
C(9)−Mo(2)−O(3)	89.0(11)
N(2)−Mo(2)−O(3)	86.5(6)
C(2)−Mo(2)−O(4)	176.1(8)
C(1)−Mo(2)−O(4)	101.4(7)
C(9)−Mo(2)−O(4)	82.6(8)
N(2)−Mo(2)−O(4)	81.2(6)
O(3)−Mo(2)−O(4)	84.3(5)
N(1)−Au(1)−P(1)	171.9(6)
N(2)−N(1)−Au(1)	127.0(14)
N(1)−N(2)−Mo(2)	120.2(13)

stopped at low temperature. In complexes **2a**, **2b**, and **3a**, (Scheme 2) the Mo−N bonds rotate freely even at 213 K, as both halves of allyl and acac ligands are equivalent in the symmetric isomer **S**, opposite to what is observed for **3b**. Although the presence of isomers such as **A** in Scheme 2 cannot be completely ruled out, the isomers detected in the NMR spectra of **3b** should be different rotamers, the Mo−N bond rotation being slow at low temperature but fast at room temperature (Scheme 3).

Therefore, rotation of the Mo−N bond, which is only detected for **3b**, is fast for the rest of the complexes described herein. As **3b** contains bulkier substituents, this leads to the conclusion that the trigonal twist rearrangement is more energetically demanding. This is easily foreseeable considering that the scrambling of coordination sites should be more difficult to achieve than a bond rotation. In **3b**, both the presence of the methyl groups in the dimethylpyrazolate and its coordination to the $AuPPh_3$ fragment cooperate to brake the rotation of the Mo−N bond, which is too fast to be detected when only one of these factors (either in **2b** or **3a**) is absent. Thus the addition of these two factors allow the "molecular brake" to be obtained.

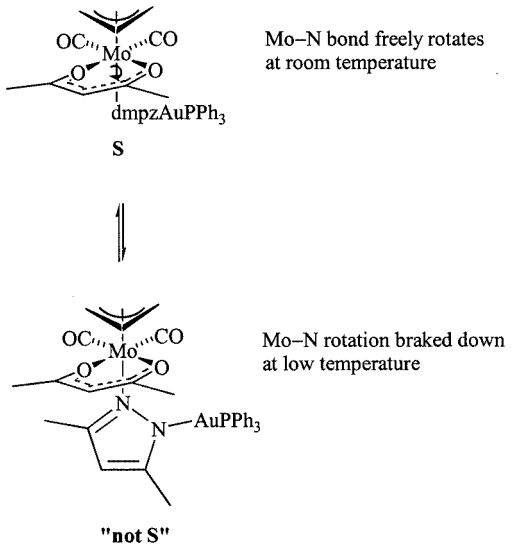

Scheme 3. Hindered rotation of the Mo−N bond observed for **3b**

Experimental Section

General Remarks: All manipulations were performed under a N_2 atmosphere following conventional Schlenk techniques. Filtrations were carried out on dry Celite under N_2. Solvents were purified according to standard procedures.[22] [Mo(η^3-allyl)Br$(CO)_2$-$(NCMe)_2$],[23] Tl(acac),[24] and [Au(acac)PPh_3][24] were obtained as described previously. All other reagents were obtained from the usual commercial suppliers, and used as received. Infrared spectra were recorded on Perkin−Elmer 1720X or RX I FT-IR apparatus on KBr pellets from 4000 to 400 cm^{-1}. NMR spectra were recorded on Bruker AC-300 or ARX-300 instruments in $CDCl_3$, at room temperature unless otherwise stated. NMR spectra are referred to the internal residual solvent peak for ^1H and $^{13}C\{^1H\}$ NMR or to external 85% aqueous H_3PO_4 for $^{31}P\{^1H\}$ NMR spectra. Assignment of the $^{13}C\{^1H\}$ NMR spectroscopic data was supported by DEPT experiments and relative intensities of the resonance signals. Elemental analyses were performed on a Perkin−Elmer 2400B microanalyzer.

[Mo(η^3-allyl)Br$(CO)_2(Hpz)_2$] (1a): [Mo(η^3-allyl)Br$(CO)_2(NCMe)_2$] (0.550 g, 1.5 mmol) was added to a solution of Hpz (0.205 g, 3 mmol) in CH_2Cl_2 (30 mL). The solution was stirred at room temperature for 5 min and hexane was added (ca. 30 mL). Concentration of the solution in vacuo and cooling to −20 °C gave a yellow microcrystalline solid, which was decanted, washed with hexane (3 × 3 mL approximately), and dried in vacuo, yielding 0.589 g (96%). IR (THF): $\tilde{\nu}$ = 1945 cm^{-1} vs, 1846 vs. IR (KBr): $\tilde{\nu}$ = 3304 cm^{-1} m, 3146 w, 3130 w, 1926 s, 1911 s, 1815 vs, 1654 vw, 1637 vw, 1466 w, 1404 vw, 1352 w, 1257 vw, 1158 vw, 1127 w, 1047 m, 911 vw, 792 w, 778 m, 719 vw, 675 vw, 602 vw, 590 vw, 502 vw. ^1H NMR (333 K, 300 MHz): 1.47 ppm (br., 2 H, H^{anti}), 3.50 (br., 2 H, H^{syn}), 4.04 (m, 1 H, H^c allyl), 6.33 (br., 2 H, H^4 Hpz), 7.39 (s, 2 H, H^3 Hpz), 7.70 (br., 1 H, H^5 Hpz), 8.10 (br., 1 H, H^5 Hpz), 11.75 (br., 2 H, *H*N). ^1H NMR (room temp., 300 MHz): 1.29 ppm (d, J = 9.2 Hz, 1 H, H^{anti}), 1.63 (d, J = 10.0 Hz, 1 H, H^{anti}), 3.19 (br., 1 H, H^{syn}), 3.84 (br., 1 H, H^{syn}), 4.03 (m, 1 H, H^c allyl), 6.25 (s, 1 H, H^4 Hpz), 6.43 (s, 1 H, H^4 Hpz), 7.40 (s, 2 H, H^3 Hpz), 7.57 (s, 1 H, H^5 Hpz), 8.37 (s, 1 H, H^5 Hpz), 11.61 (br., 1 H, *H*N), 11.78 (br., 1 H, *H*N) ppm. ^1H NMR (253 K, 300 MHz): 1.28 ppm (d, J = 9.4 Hz, 1 H, H^{anti}), 1.62 (d, J = 9.9 Hz, 1 H, H^{anti}), 3.19 (dd,

J = 6.4, 3.5 Hz, 1 H, H^{syn}), 3.82 (dd, J = 5.9, 3.5 Hz, 1 H, H^{syn}), 4.02 (m, 1 H, H^{c} allyl), 6.25 (q, J = 2.2 Hz, 1 H, H^{4} Hpz), 6.43 (q, J = 2.2 Hz, 1 H, H^{4} Hpz), 7.41 (s, 2 H, H^{3} Hpz), 7.54 (t, J = 1.8 Hz, 1 H, H^{5} Hpz), 8.39 (t, J = 1.8 Hz, 1 H, H^{5} Hpz), 11.52 (br., 1 H, HN), 11.74 (br., 1 H, HN). $^{13}C\{^{1}H\}$ NMR (room temp., 75.78 MHz): 57.5 ppm (s, CH$_2$), 63.6 (s, CH$_2$), 73.2 (s, CH allyl), 107.1 (s, C^{4}H Hpz), 107.5 (s, C^{4}H Hpz), 129.1 (s, $C^{3,5}$H Hpz), 129.2 (s, $C^{3,5}$H Hpz), 142.7 (s, $C^{5,3}$H Hpz), 144.8 (s, $C^{5,3}$H Hpz), 224.2 (s, CO), 225.1 (s, CO). $C_{11}H_{13}BrMoN_4O_2$: calcd. C 32.30, H 3.20, N 13.70; found C 32.65, H 3.08, N 13.70.

[Mo(η^3-allyl)Br(CO)$_2$(Hdmpz)$_2$] (1b): [Mo(η^3-allyl)Br(CO)$_2$(NCMe)$_2$] (0.147 g, 0.4 mmol) was added to a solution of Hdmpz (0.077 g, 0.8 mmol) in CH_2Cl_2 (15 mL). The solution was stirred at room temperature for 5 min, the volatiles were removed in vacuo, and the yellow residue was extracted with Et_2O (ca. 20 mL) and filtered. Hexane was added (ca. 20 mL) and the solution was concentrated and cooled to −20 °C, giving a yellow-orange microcrystalline solid, which was decanted, washed with hexane (3 × 3 mL approximately), and dried in vacuo, yielding 0.146 g (78%). IR (THF): $\tilde{\nu}$ = 1942 cm^{-1} vs, 1843 vs. IR (KBr): $\tilde{\nu}$ = 3294 cm^{-1}s, 3069 vw, 2994 vw, 2927 vw, 1948 s, 1930 s, 1854 vs, 1654 vw, 1636 vw, 1570 m, 1467 w, 1419 w, 1373 w, 1283 w, 1155 w, 1024 w, 799 w, 654 w, 572 vw, 512 vw, 474 vw. ^{1}H NMR (353 K, C_6D_6, 300 MHz): 1.44 ppm (br., 6 H, CH_3 Hdmpz + 2 H, H^{anti}), 2.12 (br., 3 H, CH_3 Hdmpz), 2.87 (br., 3 H, CH_3 Hdmpz), 4.20 (br., 2 H, H^{syn}), 4.32 (m, 1 H, H^{c} allyl), 5.35 (s, 2 H, H^{4} Hdmpz), 11.4 (br., 2 H, HN). ^{1}H NMR (room temp., 300 MHz): 1.25 ppm (d, J = 9.4 Hz, 1 H, H^{anti}), 1.51 (d, J = 9.9 Hz, 1 H, H^{anti}), 2.04 (s, 3 H, CH_3 Hdmpz), 2.05 (s, 3 H, CH_3 Hdmpz), 2.25 (s, 3 H, CH_3 Hdmpz), 2.95 (m partially hidden by the following signal, 1 H, H^{syn}), 2.97 (s, 3 H, CH_3 Hdmpz), 3.96 (m, 1 H, H^{syn}), 4.12 (m, 1 H, H^{c} allyl), 5.78 (s, 1 H, H^{4} Hdmpz), 5.93 (s, 1 H, H^{4} Hdmpz), 10.25 (br., 1 H, HN), 11.25 (br., 1 H, HN). ^{1}H NMR (243 K, 300 MHz): 1.26 ppm (d, J = 9.5 Hz, 1 H, H^{anti}), 1.47 (d, J = 9.8 Hz, 1 H, H^{anti}), 2.00 (s, 3 H, CH_3 Hdmpz), 2.03 (s, 3 H, CH_3 Hdmpz), 2.25 (s, 3 H, CH_3 Hdmpz), 2.91 (dd, J = 6.2, 3.3 Hz, 1 H, H^{syn}), 2.98 (s, 3 H, CH_3 Hdmpz), 3.95 (dd, J = 6.3, 3.3 Hz, 1 H, H^{syn}), 4.08 (m, 1 H, H^{c} allyl), 5.78 (s, 1 H, H^{4} Hdmpz), 5.94 (s, 1 H, H^{4} Hdmpz), 10.06 (br., 1 H, HN), 11.12 (br., 1 H, HN). $^{13}C\{^{1}H\}$ NMR (room temp., 75.78 MHz): 10.7 ppm (s, CH$_3$ Hdmpz), 10.9 (s, CH$_3$ Hdmpz), 14.1 (s, CH$_3$ Hdmpz), 15.7 (s, CH$_3$ Hdmpz), 58.8 (s, CH$_2$), 64.2 (s, CH$_2$), 75.4 (s, CH allyl), 106.5 (s, C^{4}H Hdmpz), 106.7 (s, C^{4}H Hdmpz), 139.9 (s, $C^{3,5}$ Hdmpz), 140.6 (s, $C^{3,5}$ Hdmpz), 152.2 (s, $C^{5,3}$ Hdmpz), 155.9 (s, $C^{5,3}$ Hdmpz), 224.5 (s, CO), 226.3 (s, CO). $C_{15}H_{21}BrMoN_4O_2$: calcd. C 38.73, H 4.55, N 12.04; found C 39.08, H 4.41, N 12.05.

[Mo(acac)(η^3-allyl)(CO)$_2$(Hpz)] (2a): Complex **1a** (0.245 g, 0.6 mmol) was added to a mixture of Tl(acac) (0.182 g, 0.6 mmol) in CH_2Cl_2 (30 mL) and the mixture was stirred at room temp. for 5 min. The solution was then filtered and the filtrate was evaporated to dryness. The yellowish residue was extracted with Et_2O (ca. 20 mL) and filtered. Hexane was added (ca. 30 mL) and the solution was concentrated and cooled to −20 °C, giving a yellow-orange microcrystalline solid, which was decanted, washed with hexane (3 × 3 mL approximately), and dried in vacuo, yielding 0.172 g (80%). IR (THF): $\tilde{\nu}$ = 1938 cm^{-1} vs, 1846 vs. IR (KBr): $\tilde{\nu}$ = 3159 cm^{-1} w, 1936 vs, 1842 vs, 1581 m, 1524 s, 1390 m, 1380 m, 1354 w, 1270 w, 1263 w, 1136 m, 1062 w, 1044 w, 1025 w, 932 w, 798 w, 753 w, 609 w, 571 w, 512 w. ^{1}H NMR (room temp., 300 MHz): 1.42 ppm (br., 2 H, H^{anti}), 1.90 (s, 6 H, CH_3 acac), 3.35 (br., 3 H, H^{c} allyl + H^{syn}), 5.26 (s, 1 H, CH acac), 6.40 (br., 1 H, H^{4} Hpz), 7.54 (br., 2 H, $H^{3,5}$ Hpz), 10.14 (br., 1 H, HN). ^{1}H NMR (253 K, 300 MHz): 1.18 ppm (d, J = 7.0 Hz, 1 H, H^{anti} isomer A), 1.38 (d, J = 7.6 Hz, 1 H, H^{anti} isomer A), 1.52 (d, J = 9.4 Hz, 2 H, H^{anti} isomer S), 1.89 (s, 6 H, CH_3 acac isomer S), 1.94 (s, 3 H, CH_3 acac isomer A), 1.99 (s, 3 H, CH_3 acac isomer A), 3.00 (br., 1 H, H^{syn} isomer S), 3.31 (m, 1 H, H^{syn} isomer A + 1 H, H^{c} isomer A + 1 H, H^{c} isomer S), 3.48 (br., 2 H, H^{syn} isomer S), 5.23 (s, 1 H, CH acac isomer A), 5.34 (s, 1 H, CH acac isomer S), 6.28 (s, 1 H, H^{4} Hpz isomer A), 6.52 (s, 1 H, H^{4} Hpz isomer S), 7.21 (s, 1 H, H^{3} Hpz isomer A), 7.62 (s, 1 H, H^{3} Hpz isomer S), 7.66 (s, 1 H, H^{5} Hpz isomer A), 8.20 (s, 1 H, H^{5} Hpz isomer S), 10.15 (s, 1 H, HN isomer S), 11.70 (s, 1 H, HN isomer A). Ratio isomer **A**/isomer **S** (253 K) = 1:0.7; ratio isomer **A**/isomer **S** (233 K) = 1:0.6; ratio isomer **A**/isomer **S** (213 K) = 1:0.5. $^{13}C\{^{1}H\}$ NMR (233 K, 75.78 MHz): 27.2 ppm (s, CH$_3$ acac, isomer A), 28.3 (s, CH$_3$ acac, isomer S), 28.5 (s, CH$_3$ acac, isomer A), 58.6 (s, CH$_2$, isomer A), 60.8 (s, CH$_2$, isomer A), 61.3 (s, CH$_2$, isomer S), 72.8 (s, CH allyl, isomer S), 73.0 (s, CH allyl, isomer A), 100.4 (s, CH acac, isomer S), 100.6 (s, CH acac, isomer A), 105.4 (s, C^{4}H Hpz, isomer A), 106.9 (s, C^{4}H Hpz, isomer S), 130.3 (s, $C^{3,5}$H Hpz, isomer S), 130.7 (s, $C^{3,5}$H Hpz, isomer A), 138.6 (s, $C^{5,3}$H Hpz, isomer A), 143.6 (s, $C^{5,3}$H Hpz, isomer S), 184.4 (s, CO acac, isomer A), 189.5 (s, CO acac, isomer S), 190.9 (s, CO acac, isomer A), 226.4 (s, CO, isomer A), 227.1 (s, CO, isomer A), 228.6 (s, CO, isomer S). $C_{13}H_{16}MoN_2O_4$: calcd. C 43.35, H 4.48, N 7.78; found C 43.22, H 4.36, N 8.14.

[Mo(acac)(η^3-allyl)(CO)$_2$(Hdmpz)] (2b): *Method A:* Complex **1b** (0.093 g, 0.2 mmol) was added to a mixture of Tl(acac) (0.061 g, 0.2 mmol) in CH_2Cl_2 (10 mL) and the mixture was stirred at room temp. for 45 min. The solution was then filtered and the filtrate was evaporated to dryness. The yellowish residue was extracted with Et_2O (ca. 10 mL) and filtered. Hexane was added (ca. 15 mL) and the solution was concentrated and cooled to −20 °C, giving a yellow microcrystalline solid, which was decanted, washed with hexane (3 × 3 mL approximately), and dried in vacuo, yielding 0.052 g (67%). *Method B:* Complex **1b** (0.093 g, 0.2 mmol) was added to a solution of [Au(acac)PPh$_3$] (0.112 g, 0.2 mmol) in THF (10 mL) and the mixture was stirred at room temperature for 45 min. The volatiles were removed in vacuo, and the yellow residue was extracted with hexane (15 mL) and filtered. The insoluble residue was spectroscopically identified as [AuBrPPh$_3$].[25] Concentration of the solution in vacuo and cooling to −20 °C gave a yellow microcrystalline solid, which was decanted, washed with hexane (3 × 3 mL approximately), and dried in vacuo, yielding 0.033 g (42%). IR (THF): $\tilde{\nu}$ = 1937 cm^{-1} vs, 1846 vs. IR (KBr): $\tilde{\nu}$ = 3396 cm^{-1} m, 3377 m, 2926 vw, 1927 vs, 1822 vs, 1582 s, 1526 s, 1424 w, 1391 w, 1373 m, 1272 w, 1154 w, 1026 w, 952 w, 804 w. ^{1}H NMR (room temp., 300 MHz): 1.41 ppm (br., 2 H, H^{anti}), 1.89 (s, 6 H, CH_3 acac), 2.14 (s, 3 H, CH_3 Hdmpz), 2.35 (br., 3 H, CH_3 Hdmpz), 3.31 (br., 3 H, H^{c} allyl + H^{syn}), 5.25 (br., 1 H, CH acac), 5.87 (br., 1 H, H^{4} Hdmpz), 9.12 (br., 1 H, HN). ^{1}H NMR (253 K, 300 MHz): 1.16 (d, J = 8.9 Hz, 1 H, H^{anti} isomer A), 1.36 (d, J = 9.2 Hz, 1 H, H^{anti} isomer A), 1.49 (d, J = 9.6 Hz, 2 H, H^{anti} isomer S), 1.90 (s, 6 H, CH_3 acac isomer A + 6 H, CH_3 acac isomer S), 2.14 (s, 3 H, CH_3 Hdmpz isomer A + 3 H, CH_3 Hdmpz isomer S), 2.38 (s, 3 H, CH_3 Hdmpz isomer A), 2.89 (m, 1 H, H^{c} allyl isomer A), 2.95 (s, 3 H, CH_3 Hdmpz isomer S), 3.31 (m, 2 H, H^{syn} isomer S + H^{c} allyl isomer S + 2 H, H^{syn} isomer A), 5.18 (s, 1 H, CH acac isomer S), 5.37 (s, 1 H, CH acac isomer A), 5.76 (s, 1 H, H^{4} Hdmpz isomer S), 6.01 (s, 1 H, H^{4} Hdmpz isomer A), 8.93 (s, 1 H, HN isomer A), 9.18 (s, 1 H, HN isomer S). Ratio isomer A/isomer S (253 K) = 1:0.6; ratio isomer A/isomer S (233 K) = 1:0.4; ratio isomer A/isomer S (213 K) = 1:0.2. $^{13}C\{^{1}H\}$ NMR (233 K, 75.78 MHz): 11.0 ppm (s, CH$_3$ Hdmpz, isomer A), 11.1 (s, CH$_3$ Hdmpz, isomer S),

14.0 (s, CH_3 Hdmpz, isomer A), 15.3 (s, CH_3 Hdmpz, isomer S), 27.6 (s, CH_3 acac, isomer A), 28.1 (s, CH_3 acac, isomer A), 28.3 (s, CH_3 acac, isomer S), 57.4 (s, CH_2, isomer A), 59.1 (s, CH_2, isomer A), 62.1 (s, CH_2, isomer S), 71.3 (s, CH allyl, isomer A), 72.8 (s, CH allyl, isomer S), 100.0 (s, CH acac, isomer S), 100.4 (s, CH acac, isomer A), 105.5 (s, C^4H Hdmpz, isomer A), 106.6 (s, C^4H Hdmpz, isomer S), 139.6 (s, $C^{3,5}$ Hdmpz, isomer A), 140.3 (s, $C^{3,5}$ Hdmpz, isomer S), 150.4 (s, $C^{5,3}$ Hdmpz, isomer A), 155.3 (s, $C^{5,3}$ Hdmpz, isomer S), 187.6 (s, CO acac, isomer A), 188.4 (s, CO acac, isomer A), 189.8 (s, CO acac, isomer S), 227.4 (s, CO, isomer A), 228.5 (s, CO, isomer S), 229.3 (s, CO, isomer A). $C_{15}H_{20}MoN_2O_4$: calcd. C 46.40, H 5.19, N 7.21; found C 46.09, H 4.93, N 7.09.

[Mo(acac)(η³-allyl)(CO)₂(μ-pz)AuPPh₃] (3a): Complex **2a** (0.090 g, 0.25 mmol) was added to a solution of [Au(acac)PPh_3] (0.140 g, 0.25 mmol) in THF (20 mL) and the solution, which rapidly turned orange, was stirred at room temperature for 5 min. The volatiles were removed in vacuo and the yellow residue was extracted in CH_2Cl_2/hexane (20:20 mL) and filtered. Concentration in vacuo and cooling to −20 °C gave a orange microcrystalline solid, which was decanted, washed with hexane (3 × 3 mL approximately), and dried in vacuo, yielding 0.154 g (72%) of **3a**·0.5CH_2Cl_2. IR (THF): $\tilde{\nu}$ = 1928 cm^{-1} vs, 1830 vs. IR (KBr): $\tilde{\nu}$ = 3059 cm^{-1} vw, 2991 vw, 1924 vs, 1824 vs, 1586 m, 1568 m, 1529 m, 1492 vw, 1481 vw, 1437 m, 1985 m, 1378 m, 1269 w, 1174 vw, 1162 vw, 1102 m, 1076 vw, 1055 w, 1026 w, 998 vw, 750 w, 748 w, 712 w, 696 m, 546 m, 513 w, 500 w. ^1H NMR (room temp., 300 MHz): 1.35 ppm (m, 2 H, H^{anti}), 1.72 (br., 6 H, CH_3 acac), 2.8−3.7 (br., 3 H, H^c allyl + H^{syn}), 4.97 (s, 1 H, CH acac), 6.17 (br., 1 H, H^4 pz), 7.20 (br., 1 H, H^3 pz), 7.3−7.9 (br., 16 H, C_6H_5 + H^5 pz). ^1H NMR (253 K, 300 MHz): 1.13 ppm (d, J = 8.8 Hz, 1 H, H^{anti} isomer A), 1.38 (d, J = 8.8 Hz, 1 H, H^{anti} isomer A), 1.43 (d, J = 8.3 Hz, 2 H, H^{anti} isomer S), 1.65 (s, 3 H, CH_3 acac isomer A), 1.75 (s, 6 H, CH_3 acac isomer S), 1.80 (s, 3 H, CH_3 acac isomer A), 2.94 (br., 2 H, H^{syn} isomer S), 3.38 (br., 1 H, H^c allyl isomer S + 1 H, H^{syn} isomer A), 3.55 (m, 1 H, H^c allyl isomer A + 1 H, H^{syn} isomer A), 4.96 (s, 1 H, CH acac isomer A), 5.12 (s, 1 H, CH acac isomer S), 6.14 (s, 1 H, H^4 pz isomer A), 6.28 (s, 1 H, H^4 pz isomer S), 7.15 (s, 1 H, H^3 pz isomer A), 7.22 (s, 1 H, H^3 pz isomer S), 7.37 (s, 1 H, H^5 pz isomer A), 7.4−7.9 (m, 15 H, C_6H_5 both isomers + 1 H, H^5 pz isomer S). Ratio isomer A/isomer S (253 K) = 1:0.5; ratio isomer A/isomer S (233 K) = 1:0.6; ratio isomer A/isomer S (213 K) = 1:0.7. $^{31}P\{^1H\}$ NMR (room temp., 121.49 MHz): 31.1 ppm (s, PPh_3). $^{31}P\{^1H\}$ NMR (213 K, 121.49 MHz): 33.6 ppm (s, PPh_3 isomer S), 39.3 (s, PPh_3 isomer A). $C_{63}H_{62}Au_2Cl_2Mo_2N_4O_8P_2$ (**3a**·0.5CH_2Cl_2): calcd. C 43.95, H 3.63, N 3.25; found C 43.62, H 3.52, N 3.20.

[Mo(acac)(η³-allyl)(CO)₂(μ-dmpz)AuPPh₃] (3b): *Method A:* Complex **2b** (0.039 g, 0.1 mmol) was added to a solution of [Au(acac)PPh_3] (0.056 g, 0.1 mmol) in THF (10 mL) and the solution, which rapidly turned orange, was stirred at room temperature for 5 min. The volatiles were removed in vacuo and the yellow residue was extracted in CH_2Cl_2/hexane (15:15 mL) and filtered. Concentration in vacuo and cooling to −20 °C gave a deep orange microcrystalline solid, which was decanted, washed with hexane (3 × 3 mL approximately), and dried in vacuo, yielding 0.055 g (65%). *Method B:* Complex **1b** (0.093 g, 0.2 mmol) was added to a solution of [Au(acac)PPh_3] (0.224 g, 0.4 mmol) in THF (10 mL) and the solution was stirred at room temp. for 1 h. The volatiles were removed in vacuo and the yellow residue was extracted in hexane/toluene (20:10 mL) and filtered. The insoluble residue was spectroscopically identified as [$AuBrPPh_3$].[25] The filtrate was evaporated to dryness and extracted in CH_2Cl_2/hexane (10:10 mL). Concentration in vacuo and cooling to −20 °C gave a deep orange microcrystalline solid, which was decanted, washed with hexane (3 × 3 mL

Table 3. Crystal data and refinement details for **1a**, **1b**, and **3b**

	Compound **1a**	Compound **1b**	Compound **3b**
Empirical formula	$C_{11}H_{13}BrMoN_4O_2$	$C_{15}H_{21}BrMoN_4O_2$	$C_{33}H_{34}AuMoN_2O_4P$
Formula mass	409.10	465.21	846.50
Crystal system	monoclinic	orthorhombic	triclinic
Space group	$P2_1/n$ (No. 14)	$P2_12_12_1$ (No. 19)	$P\bar{1}$ (No. 2)
a [Å]	8.368(1)	14.017(6)	8.142(4)
b [Å]	12.448(2)	14.739(6)	12.328(6)
c [A]	13.810(2)	18.347(7)	16.491(8)
α [deg]	90	90	77.122(8)
β [deg]	90.317(2)	90	84.196(9)
γ [deg]	90	90	81.489(7)
V [Å^3]	1.438.5(3)	3790.6(3)	1591.9(13)
Z	4	8	2
T [K]	293	293	293
d_{calc} [g cm^{-3}]	1.889	1.630	1.766
F(000)	800	1856	828
λ [Mo-$K_α$) [Å]	0.71073	0.71073	0.71073
Crystal size [mm]; color	0.15 × 0.15 × 0.10, yellow	0.25 × 0.17 × 0.15, yellow	0.16 × 0.06 × 0.02, orange
μ [mm^{-1}]	3.692	2.813	5.086
Scan range [deg]	2.2 ≤ θ ≤ 23.3	1.8 ≤ θ ≤ 23.3	1.3 ≤ θ ≤ 23.3
Absorption correction	SADABS	SADABS	SADABS
Corr. factors (min, max)	1.000, 0.725	1.000, 0.800	1.000, 0.646
Number of measured refelections	6182	17322	10236
Number of independent reflections [R(int)]	2063 (0.0235)	5470 (0.0316)	4570 (0.0983)
Number of observed reflections, $I \geq 2\sigma(I)$	1833	4880	2237
GOF on F^2	1.008	1.031	1.065
Number of parameters	180	424	371
Residuals R, $wR2$	0.0195, 0.0480	0.0225, 0.0403	0.0641, 0.1325

approximately), and dried in vacuo, yielding 0.073 g (43%). IR (THF): $\tilde{\nu}$ = 1924 cm^{-1} vs, 1825 vs. IR (KBr): $\tilde{\nu}$ = 3055 cm^{-1} w, 2990 w, 2914 w, 1913 vs, 1816 vs, 1585 s, 1521 s, 1482 w, 1437 m, 1393 m, 1374 m, 1264 w, 1184 vw, 1136 vw, 1102 m, 1020 w, 998 vw, 934 vw, 749 w, 712 w, 694 m, 545 m, 508 m. ^{1}H NMR (room temp., 300 MHz): 1.39 ppm (br., 2 H, H^{anti}), 1.60 (s, 6 H, CH_3 acac), 2.37 (s, 6 H, CH_3 dmpz), 3.27 (br., 1 H, H^c allyl), 3.38 (br., 2 H, H^{syn}), 4.80 (br., 1 H, CH acac), 5.88 (br., 1 H, H^4 dmpz), 7.52 (br., 10 H, C_6H_5,), 7.71 (br., 5 H, C_6H_5). ^{1}H NMR (213 K, 300 MHz, Major isomer): 1.37 ppm (d, J = 9.2 Hz, 1 H, H^{anti}), 1.44 (d, J = 8.9 Hz, 1 H, H^{anti}), 1.53 (s, 3 H, CH_3 acac), 1.69 (s, 3 H, CH_3 acac), 2.38 (s, 3 H, CH_3 dmpz), 2.40 (s, 3 H, CH_3 dmpz), 3.19 (m, 1 H, H^c allyl), 3.29 (br., 1 H, H^{syn}), 3.43 (br., 1 H, H^{syn}), 4.81 (s, 1 H, CH acac), 5.93 (s, 1 H, H^4 dmpz), 7.32 (m, 10 H, C_6H_5), 7.67 (m, 5 H, C_6H_5). Ratio major isomer/minor isomers = 1:0.3. ^{31}P{^{1}H} NMR (room temp., 121.49 MHz): 31.40 ppm (s, PPh$_3$). ^{31}P{^{1}H} NMR (213 K, 121.49 MHz): 30.4 (s, PPh$_3$, minor isomer), 30.6 (s, PPh$_3$, minor isomer), 31.0 (s, PPh$_3$, major isomer), 31.6 (s, PPh$_3$, minor isomer), 32.4 (s, PPh$_3$, minor isomer), 43.3 (s, PPh$_3$, minor isomer). The ^{1}H and ^{31}P{^{1}H} NMR spectra recorded at 213 K of a sample obtained immediately after mixing the solid complex and frozen $CDCl_3$ at −78 °C showed only signals of the major isomer. $C_{33}H_{34}AuMoN_2O_4P$: calcd. C 46.82, H 4.05, N 3.31; found C 46.45, H 3.85, N 3.05.

X-ray Crystallographic Study of 1a, 1b, and 3b: Crystals were grown by slow diffusion of hexane into concentrated solutions of the complexes in CH_2Cl_2 at −20 °C. Relevant crystallographic details are given in Table 3. A crystal was attached to a glass fiber and transferred to a Bruker AXS SMART 1000 diffractometer with graphite monochromatized Mo-K_α X-radiation and a CCD area detector. A hemisphere of the reciprocal space was collected up to 2θ = 48.6°. Raw frame data were integrated with the SAINT program.[26] The structure was solved by direct methods with SHELXTL.[27] A semi-empirical absorption correction was applied with the program SADABS.[28] All non-hydrogen atoms were refined anisotropically. Hydrogen atoms were set in calculated positions and refined as riding atoms, with a common thermal parameter. All calculations and graphics were made with SHELXTL. CCDC-189498 (**1a**), −189499 (**1b**), and −189500 (**3b**) contain the supplementary crystallographic data for this paper. These data can be obtained free of charge at www.ccdc.cam.ac.uk/conts/retrieving.html [or from the Cambridge Crystallographic Data Centre, 12, Union Road, Cambridge CB2 1EZ, UK; fax: (internat.) +44−1223/336-033; E-mail: deposit@ccdc.cam.ac.uk].

Acknowledgments

We thank the D.G.I.C.Y.T. (PB97 0470-C02-01) and the J.C.yL. (VA, 32/00B) for financial support.

[1] [1a] J. Reedijk, in: *Comprehensive Coordination Chemistry* (Eds.: G. Wilkinson, R. D. Gillard, J. A. McCleverty); Pergamon, Oxford, UK, **1987**; vol. 2., chapter 13.2.[1b]S. Trofimenko, *Prog. Inorg. Chem.* **1986**, *34*, 115−210. [1c] G. La Monica, G. A. Ardizzoia, *Prog. Inorg. Chem.* **1997**, *46*, 151−238.

[2] Some recent leading references: [2a] J. Barberá, A. Elduque, R. Giménez, L. A. Oro, J. L. Serrano, *Angew. Chem. Int. Ed. Engl.* **1996**, *35*, 2832−2835. [2b] C. Tejel, M. A. Ciriano, A. J. Edwards, F. J. Lahoz, L. A. Oro, *Organometallics* **1997**, *16*, 45−53. [2c] C. Tejel, M. A. Ciriano, J. A. López, F. J. Lahoz, L. A. Oro, *Organometallics* **1997**, *16*, 4718−4727. [2d] C. Tejel, M. A. Ciriano, J. A. López, F. J. Lahoz, L. A. Oro, *Angew. Chem. Int. Ed. Eng.* **1998**, *37*, 1542−1545. [2e] G. A. Ardizzoia, S. Cenini, G. La Monica, N. Masciocchi, A. Maspero, M. Moret, *Inorg. Chem.* **1998**, *37*, 4284−4292. [2f] C. Tejel, M. A. Ciriano, L. A. Oro, *Chem. Eur. J.* **1999**, *5*, 1131−1135. [2g] H. Matsushima, H. Hamada, K. Watanabe, M. Koikawa, T. Tokii, *J. Chem. Soc., Dalton Trans.* **1999**, 971−977. [2h] S. Komeda, M. Lutz, A. L. Spek, M. Chikuma, J. Reedijk, *Inorg. Chem.* **2000**, *39*, 4230−4236. [2i] E. Sola, F. Torres, M. V. Jiménez, J. A. López, S. E. Ruiz, F. J. Lahoz, A. Elduque, L. A. Oro, *J. Am. Chem. Soc.* **2001**, *123*, 11925−11932.

[3] See for example: [3a] L. A. Oro, D. Carmona, J. Reyes, C. Foces-Foces, F. H. Cano, *J. Chem. Soc., Dalton Trans.* **1986**, 31−37. [3b] D. Carmona, J. Ferrer, F. J. Lahoz, L. A. Oro, J. Reyes, M. Esteban, *J. Chem. Soc., Dalton Trans.* **1991**, 2811−2820. [3c] G. López, J. Ruiz, C. Vicente, J. M. Martí, G. García, P. A. Chaloner, P. B. Hitchcock, R. M. Harrison, *Organometallics* **1992**, *11*, 4090−4096. [3d] D. Carmona, J. Ferrer, R. Atencio, F. J. Lahoz, L. A. Oro, M. P. Lamata, *Organometallics* **1995**, *14*, 2057−2065. [3e] G. A. Ardizzoia, G. La Monica, A. Maspero, N. Masciocchi, M. Moret, *Eur. J. Inorg. Chem.* **1999**, 1301−1307. [3f] G. A. Ardizzoia, G. La Monica, A. Maspero, M. Moret, N. Masciocchi, *Eur. J. Inorg. Chem.* **2000**, 181−187. [3g] R. Contreras, M. Valderrama, E. M. Orellana, D. Boys, D. Carmona, L. A. Oro, M. P. Lamata, J. Ferrer, *J. Organomet. Chem.* **2000**, *606*, 197−202.

[4] [4a] P. Braunstein, J. Rose, in: *Comprehensive Organometallic Chemistry II* (Eds.: E. W. Abel, F. G. A. Stone, G. Wilkinson); Pergamon, Oxford, UK, **1995**; vol. 10, Ed. R. D. Adams, chapter 7. [4b]N. Wheatley, P. Kalck, *Chem. Rev.* **1999**, *99*, 3379−3419. [4c] R. D. Adams, *J. Organomet. Chem.* **2000**, *600*, 1−6.

[5] M. D. Curtis, O. Eisenstein, *Organometallics* **1984**, *3*, 887−895.

[6] J. W. Faller, D. A. Haitko, R. D. Adams, D. F. Chodosh, *J. Am. Chem. Soc.* **1979**, *101*, 865−876.

[7] [7a] S. K. Chowdhury, M. Nandi, V. S. Joshi, A. Sarker, *Organometallics* **1997**, *16*, 1806−1809. [7b] D. S. Frohnapfel, P. S. White, J. L. Templeton, H. Rüegger, P. S. Pregosin, *Organometallics* **1997**, *16*, 3737−3750. [7c] K.-B. Shiu, C.-J. Chang, Y. Wang, M.-C. Cheng, *J. Organomet. Chem.* **1991**, *406*, 363−369.

[8] P. Espinet, R. Hernando, G. Iturbe, F. Villafañe, G. A. Orpen, I. Pascual, *Eur. J. Inorg. Chem.* **2000**, 1031−1038.

[9] [9a] D. Carmona, L. A. Oro, M. P. Lamata, J. Elguero, M. C. Apreda, C. Foces-Foces, F. H. Cano, *Angew. Chem. Int. Ed. Engl.* **1986**, *25*, 1114−1115. [9b] D. Carmona, J. Ferrer, L. A. Oro, M. C. Apreda, C. Foces-Foces, F. H. Cano, J. Elguero, M. L. Jimeno, *J. Chem. Soc., Dalton Trans.* **1990**, 1463−1476. [9c] D. Röttger, G. Erker, M. Grehl, R. Fröhlich, *Organometallics* **1994**, *13*, 3897−3902. [9d] D. Carmona, J. Ferrer, J. M. Arilla, J. Reyes, F. J. Lahoz, S. Elipe, F. J. Modrego, L. A. Oro, *Organometallics* **2000**, *19*, 798−808.

[10] T. Beringhelli, G. D'Alonso, M. Panigati, F. Porta, P. Mercandelli, M. Moret, A. Sironi, *Organometallics* **1998**, *17*, 3282−3292.

[11] [11a] R. Davis, L. A. P. Kane-Maguire, in: *Comprehensive Organometallic Chemistry* (Eds.: G. Wilkinson, F. G. A. Stone, E. W. Abel); Pergamon, Oxford, UK, **1982**, vol. 8; 1156−1159. [11b] M. W. Whiteley, in: *Comprehensive Organometallic Chemistry II* (Eds.: E. W. Abel, F. G. A. Stone, G. Wilkinson); Pergamon, Oxford, UK, **1995**. vol. 12 (Eds.: J. A. Labinger, M. J. Winter); pp. 337−338.

[12] F. A. Cotton, R. L. Luck, *Acta Crystallogr., Sect. C* **1990**, *46*, 138−140.

[13] G. A. Jeffrey, *An Introduction to Hydrogen Bonding*; Oxford University Press, New York, **1997**, chapter 2.

[14] [14a] G. A. Ardizzoia, G. LaMonica, A. Maspero, M. Moret, N. Masciocchi, *Eur. J. Inorg. Chem.* **1998**, 1503−1511. [14b] J. Cámpora, J. A. López, C. M. Maya, P. Palma, E. Carmona, C. Ruiz, *Organometallics* **2000**, *19*, 2707−2715.

[15] [15a] B. M. Trost, M. Lautens, *J. Am. Chem. Soc.* **1982**, *104*, 5543−5545. [15b] B. M. Trost, M. Lautens, *J. Am. Chem. Soc.* **1987**, *109*, 1469−1478. [15c] B. M. Trost, C. A. Merlic, *J. Am.*

Chem. Soc. **1990**, *112*, 9590−9600. [15d] M. P. T. Sjögren, H. Frisell, B. Åkermark, P.-O. Norrby, L. Eriksson, A. Vitagliano, *Organometallics* **1997**, *16*, 942−950. [15e] B. M. Trost, I. Hachiya, *J. Am. Chem. Soc.* **1998**, *120*, 1104−1105.

[16] [16a] J. W. Faller, D. Linebarrier, *Organometallics* **1988**, *7*, 1670−1672. [16b] J. Pérez, L. Riera, V. Riera, S. García-Granda, E. García-Rodríguez, *J. Am. Chem. Soc.* **2001**, *123*, 7469−7470.

[17] A. T. T. Hsieh, B. O. West, *J. Organomet. Chem.* **1976**, *112*, 285−296.

[18] A referee has drawn our attention to the fact that the different populations of isomers **S** in complexes **1** and **2** could be related to the ligand *trans* to the allyl: pyrazole for **2**, but Br for **1**. In fact, there is a clear preference for the pyrazole against the bromo ligand in complexes **1**, whereas a more balanced competition between acac and the pyrazole seems to take place in complexes **2**.

[19] Ref.[13] paragraph 11.2.

[20] B. J. Brisdon, A. A. Woolf, *J. Chem. Soc., Dalton Trans.* **1978**, 291−295.

[21] F. Bachechi, A. Burini, R. Galassi, B. R. Pietroni, M. Severini, *J. Organomet. Chem.* **1999**, *575*, 269−277.

[22] D. D. Perrin, W. L. F. Armarego, *Purification of Laboratory Chemicals*; 3rd ed.; Pergamon Press: Oxford, **1988**.

[23] H. Tom Dieck, H. Friedel, *J. Organomet. Chem.* **1968**, *14*, 375−385.

[24] J. Vicente, M. T. Chicote, *Inorg. Synth.* **1998**, *32*, 172−177.

[25] P. F. Barron, L. M. Engelhardt, P. C. Healy, J. Oddy, A. H. White, *Aust. J. Chem.* **1987**, *40*, 1545−1555.

[26] *SAINT+.SAX* area detector integration program. Version 6.02. Bruker AXS, Inc., Madison, WI, **1999**.

[27] G. M. Sheldrick; *SHELXTL*, An integrated system for solving, refining, and displaying crystal structures from diffraction data. Version 5.1. Bruker AXS, Inc. Madison, WI, **1998**.

[28] G. M. Sheldrick; *SADABS*, Empirical Absorption Correction Program. University of Göttingen: Göttingen, Germany, **1997**.

Received July 15, 2002
[I02387]